Pn TOMOGRAPHY, GEOPHYSICAL MODELS, CROSS CORRELATION, AND LOCATION IN EURASIA

Lee K. Steck[1], Hans E. Hartse[1], Monica Maceira[1], Jonathan K. MacCarthy[1], Charlotte A. Rowe[1], W. Scott Phillips[1], Kevin G. Mackey[2], Kazuya Fujita[2], Michael L. Begnaud[1], and Diane F. Baker[1]

Los Alamos National Laboratory[1] and Michigan State University[2]

Sponsored by National Nuclear Security Administration
Office of Nonproliferation Research and Development
Office of Defense Nuclear Nonproliferation

Contract Nos. W-7405-ENG-36[1] and DE-FC52-2004NA25540[2]

ABSTRACT

This paper covers several facets of the location and geophysical modeling efforts at Los Alamos National Laboratory (LANL). In location we continue to develop kriged correction surfaces for Eurasian stations and show results from relocations of GT25 or better events using small (3 to 10 station) regional networks in Asia. With empirical corrections, locations for 70% of tested events were improved using first P only, while 82% improved using first P and first S arrivals. We are exploring model-based corrections using velocity models derived from Pn tomography of China and Siberia. Relocations in Asia using travel times calculated from Pn velocity perturbations show a 10-30% improvement over IASPEI91 travel times alone; similar tests will be performed in northeastern Asia. Pn tomography in northeastern Asia indicates higher velocities under the Siberian platform, with generally lower velocities under regions of more active tectonics. In Central Asia, we are using correlation repicking, satellite imagery and pattern recognition software to identify potential mines and tie correlated seismic events to mining locations. The pattern recognition software has identified several mining locations that we are linking to clusters of correlated seismic events, which are identified from the Kazakh National Data Center (KNDC) bulletins. For geophysical models, we have recently developed a new joint inversion method using gravity and surface wave group velocity data. This method has been applied to the Tarim and Junggar basins and shows high upper mantle velocities beneath the Tarim, with differences in lower-crust and upper-mantle shear velocities between the eastern and western Tarim.

OBJECTIVES

The objective of these studies is to improve our ability to locate and discriminate seismic events in Asia. Our approach relies on the acquisition of ground truth (GT) for empirical corrections and the development of regional velocity models upon which travel time, azimuth, and slowness correction surfaces can be built. In this paper we present results from model development in Siberia and the Tarim Basin, identification of mining explosions in central Asia, and regional station calibration in Asia.

RESEARCH ACCOMPLISHED

Regional Station Calibration in Asia

We are exploring the location performance of small, poorly configured regional seismic networks in Asia. Our stations have been calibrated using GT ranging from 1 km to 25 km, and typical relocations involved from 3 to 12 stations using both primary and secondary phases. Stations and events used in the tests are shown in Figure 1. Network performance is shown in Figures 2 and 3.

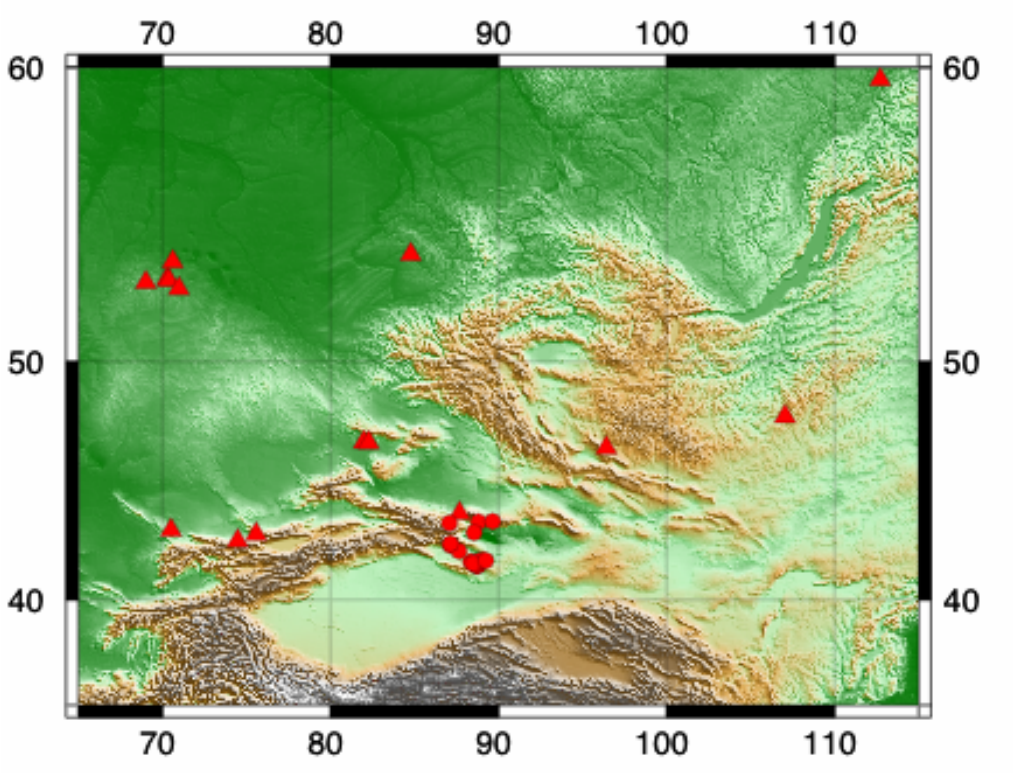

Figure 1. Stations (triangles) and events (circles) used in our tests.

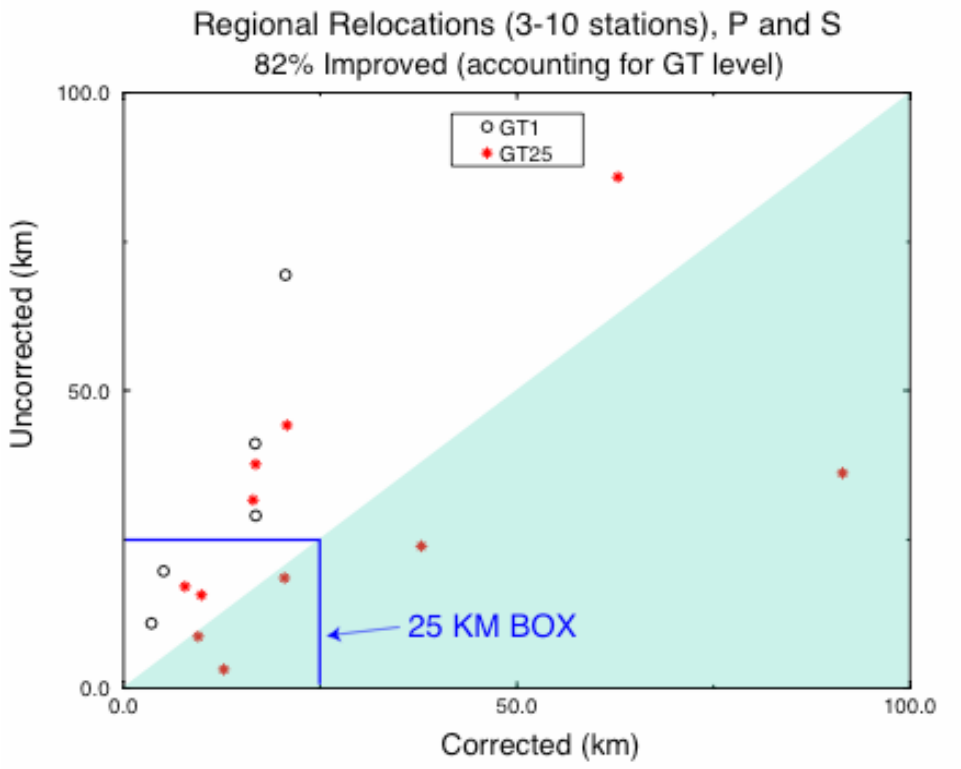

Figure 2. Network performance comparing mislocations using kriged travel time correction surfaces to mislocations with no corrections.

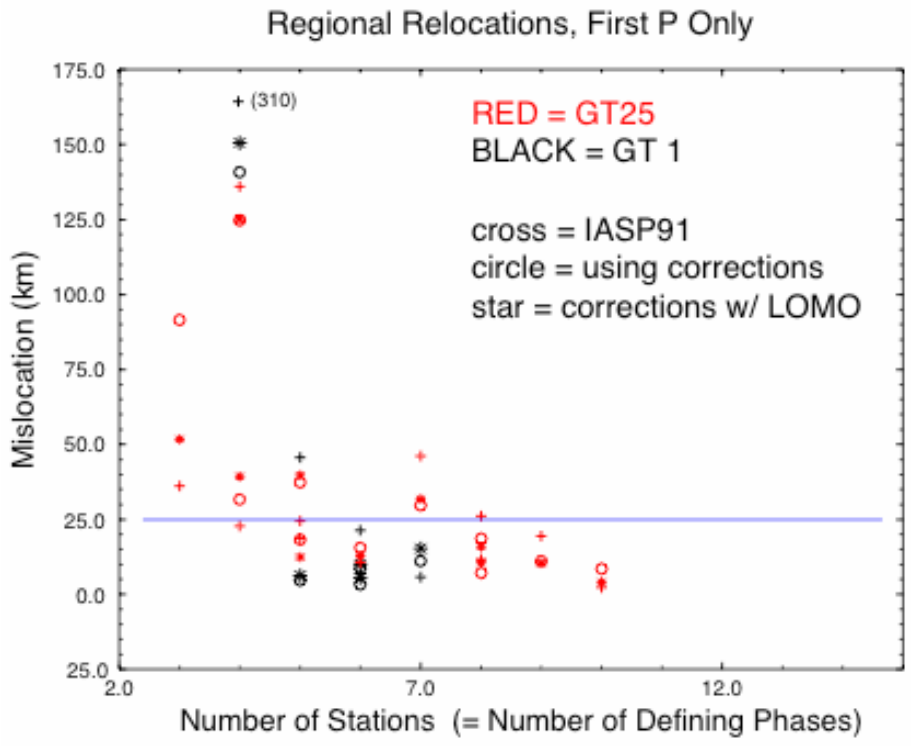

Figure 3. Mislocations with IASPEI91 only (crosses), kriged correction surfaces (circles), and leave-one-out relocations with correction surfaces (stars). In these tests, only first P was used. The blue line indicates a mislocation of 25 km.

Pn Tomography of Siberia

We have applied the method of Phillips et al. (2005) to invert for Pn velocities in Siberia (Steck et al., 2005). We apply the technique to events from the Michigan State University eastern Russia seismic database, following a relocation of the full catalog within a consistent base model (IASPEI91) and incorporation and association of phase arrivals from other sources where applicable. For this study we restrict our test to source-receiver distance of 2 – 20 degrees. The eastern Russia database provides us with differential raypaths for 459 stations, yielding 27,291 station pair combinations with a catalog of 65,489 earthquakes between 45° and 80° N, 100° to 175° E. This resulted in 666,387 differential paths from which to invert for the Pn slowness perturbations and station corrections. Pn tomography in northeastern Russia indicates higher velocities under the Siberian platform, with generally lower velocities under regions of more active tectonics (Figure 4).

Joint Inversion of Surface Wave and Gravity Data in the Tarim Basin

We implement and apply a method to jointly invert surface-wave group velocities and free-air gravity observations. Surface-wave dispersion measurements are sensitive to seismic shear-wave velocities, and the gravity measurements supply constraints on rock density variations. Our goal is to obtain a self-consistent three-dimensional shear-velocity-density model with increased resolution of shallow geologic structures. To obtain the 3-D shear-wave velocity model we parameterize it in terms of one-dimensional (1-D), depth-dependent velocity profiles determined at the center of each cell in a grid of 1° by 1°. In each cell we consider two sets of data points: fundamental-mode group velocities and free-air gravity anomalies. Our approach to joint inversion is very similar and basically follows the scheme described by Julià et al. (2000), except for the implementation of gravity anomaly contributions.

We apply the method to investigate the structure of the crust and upper mantle beneath two large central Asia sedimentary basins: the Tarim and Junggar. The basins have thick sediment sections that produce substantial

regional gravity variations (up to several hundred mGal). We used gravity observations extracted from the global gravity model derived from the Gravity Recovery and Climate Experiment (GRACE) satellite mission (Tapley et al., 2005). We combine the gravity anomalies with high-resolution surface-wave slowness tomographic maps that provide group velocity dispersion values in the period range between 8 and 100 s for a grid of locations across central Asia. To integrate these data, we use a relationship between seismic velocity and density constructed through the combination of two empirical relations: one determined by Nafe and Drake (1963), most appropriate for sedimentary rocks, and a linear Birch's Law (Birch, 1961) more applicable to denser rocks (the basement) (Figure 4). An iterative, damped least squares inversion including smoothing is used to jointly model both data sets, using shear-velocity variations as the primary model parameters.

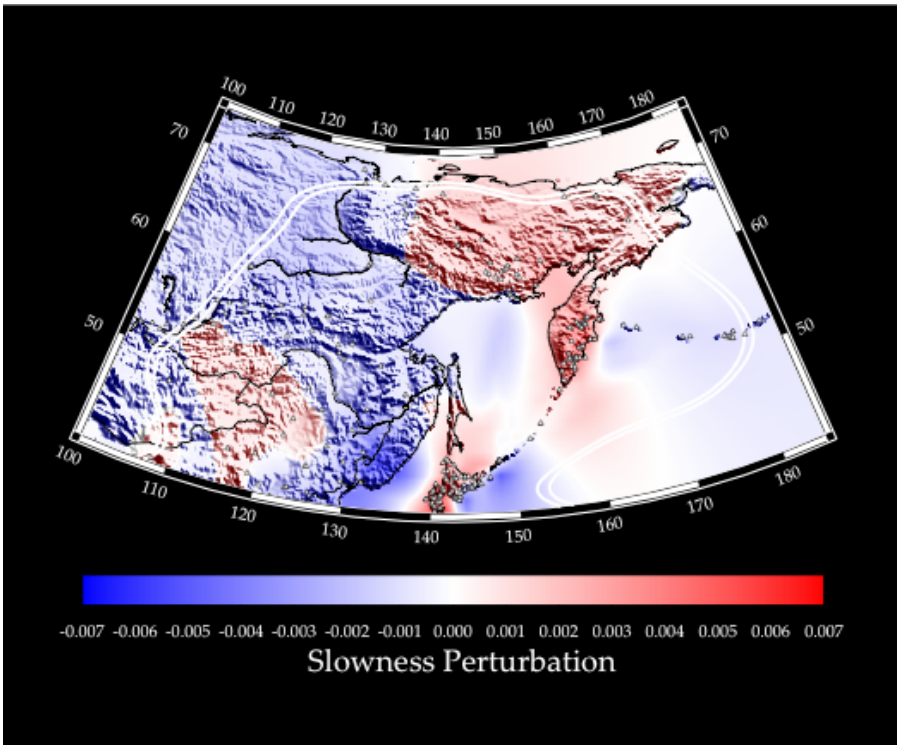

Figure 4. Pn tomography results for northeastern Russia from Rowe et al., 2006.

Results show high upper-mantle shear velocities beneath the Tarim basin and suggest differences in lower-crust and upper-mantle shear velocities between the eastern and western Tarim (Figure 5). At shallow depths, the images are dominated by slow velocities in the Tarim and Junggar basins. This is a predictable result because of the clear presence of low velocities associated with the known major sedimentary basins in the tomographic images at short periods (Maceira et al., 2005). However, the seismic structure in these basins shows slower velocities than without including the gravity in the inversion process. We think that this is an improvement of our 3-D model since seismic discrimination has proven the need for slower velocities at shorter periods (i.e., shallower layers) in those sedimentary basins (see Acknowledgements). Velocity images at mid-crustal depths show differences between eastern and western Tarim. Deeper in the crust and upper mantle, fast velocity regions are found beneath the basins. This is usually interpreted as an indication of old, cold, thick lithospheric blocks that have not been greatly deformed or modified by tectonic activity since their emplacement. The upper mantle velocity slice at 55-km depth shows once more differences between the east and west part of the Tarim basin. In this case, western Tarim displays faster velocities than the eastern side, in good agreement with previous observations (Liang and Song, 2004; Sun and Toksöz, 2006). Depth slices at deeper depths are somewhat puzzling. It could be that the near-surface model cannot explain the higher wavenumber data in the GRACE observations and these then get mapped to greater depths where constraints are weaker. Future work will seek even better models. This could be accomplished by reducing the grid sampling and using many more cells or with additional lateral smoothing with depth (based on the wavelengths that sample those depths). The value of jointly inverting surface wave and gravity data is clear (Figure 6). It is well known that traditional inversion techniques of surface wave dispersion data for seismic structure suffer from poor

resolution and non-uniqueness, especially when a single surface wave mode is used. Joint inversion approaches can help alleviate the problem (Figure 7).

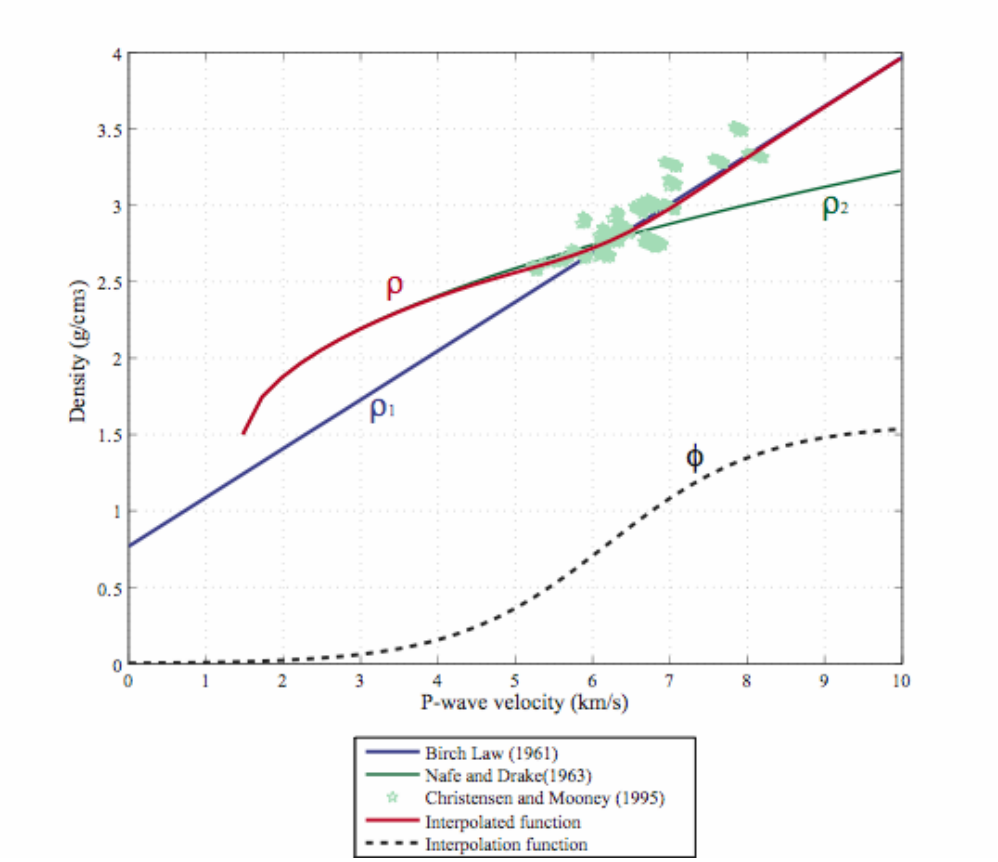

Figure 5. Relationships between P-wave velocity and density used in this study. The solid green line is Onizawa et al. (2002) polynomial fit to laboratory measurements on sediments and sedimentary rocks summarized by Nafe and Drake (1963). The solid blue line is the empirical linear relationship known as Birch's law (1961). Using the interpolation function represented by the dashed black line, we constructed our own relationship by combination of the two empirical ones. The interpolated function is represented by the solid red line. Light green stars are rock measurements performed by Christensen and Mooney (1995) at different depths and temperatures.

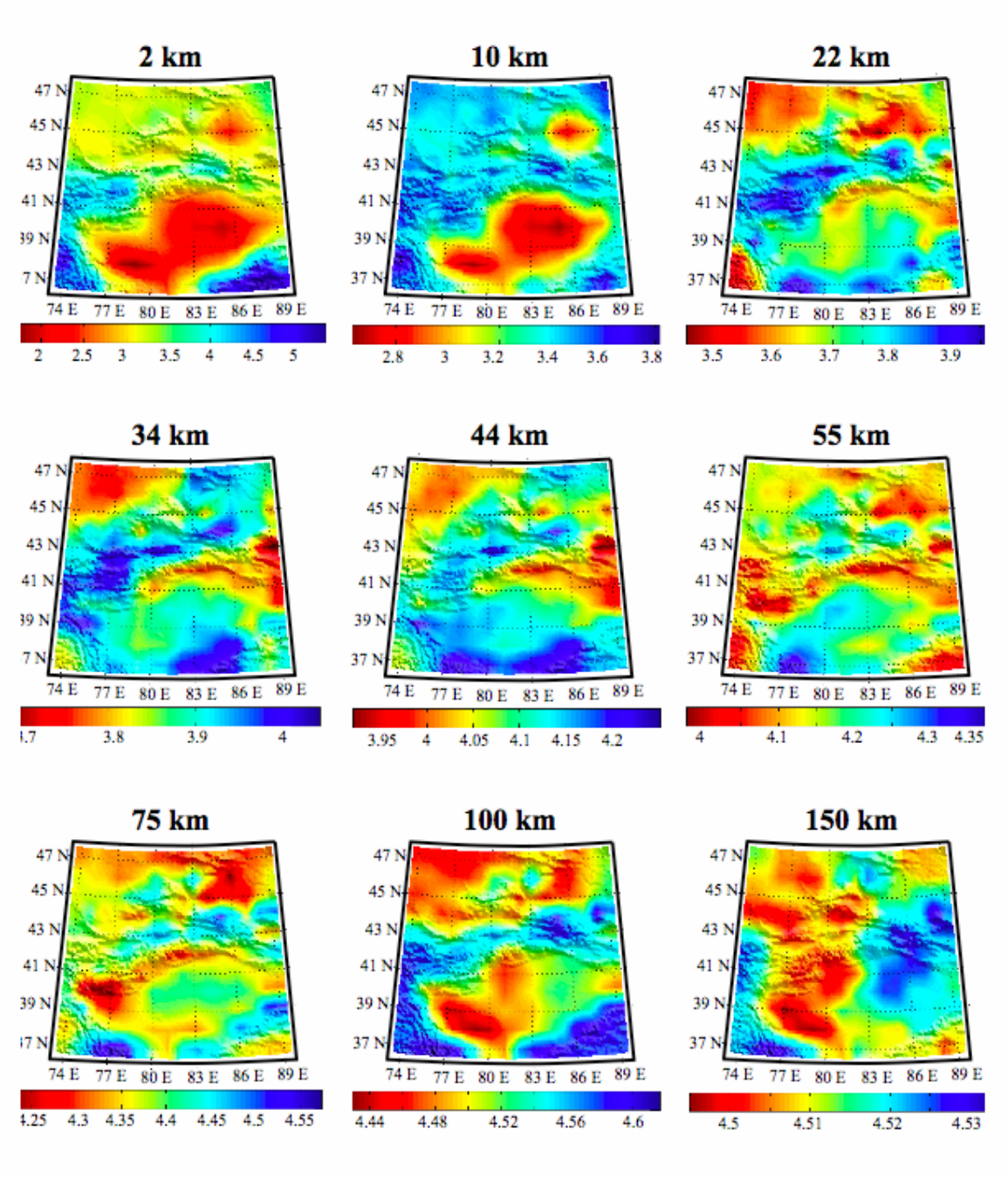

Figure 6. S-wave velocity model at constant depth slices. The depth of each image is shown at the top of each map. Velocity values are expressed in km/s. Note the color scheme is different for each image.

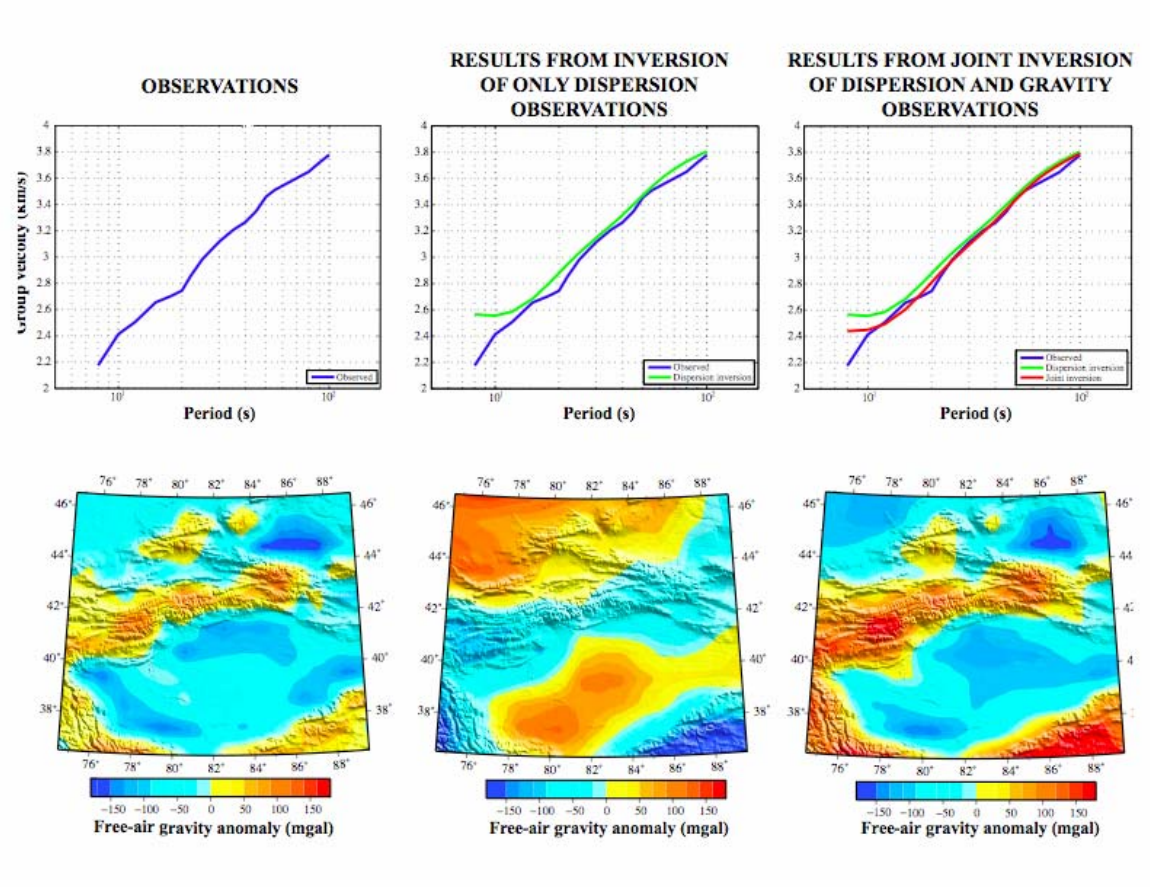

Figure 7. Comparison of data fits from the inversion of only surface wave dispersion observations and from the joint inversion of dispersion and gravity observations. Top panels from left to right: surface wave dispersion data for a typical cell (blue line); fit to the dispersion data from inverting only dispersion data (green line); fit to the dispersion data from the joint inversion (red line). Bottom panels from left to right: GRACE data for the region under study; predicted free-air gravity anomalies from the model resulting from inverting only dispersion observations; predicted free-air gravity anomalies from the model resulting from the joint inversion.

Mining Explosions in Central Asia

In this effort we are exploring the combined use of correlation arrival time picking using the cross-coherency-correlation method of Rowe et al. (2002) and the clustering/stacking approach of Rowe et al. (2004), in combination with satellite imagery to identify mining locations and repeating events in central Asia. The goals of this effort are: (1) build seismicity catalogs of GT mining explosions, (2) create libraries of mine images, (3) create libraries of reference waveforms to accommodate the catalogs and images. Figure 8 shows bins of event origin time-of-day reported in Kazakh National Data Center bulletins and reveals areas where presumed man-made sources dominate the seismicity (gold and yellow bins). By identifying highly correlated waveforms at both array MKAR and station KURK we have identified events whose origins must be similarly located (Figure 9). Relocations of the events using the cross correlation re-picks identifies tight clusters that can be tied to mine locations (Figure 10). We are using a pattern recognition algorithm, GENIEPro, trained on known mining sites (Figure 11), to identify new mine locations in satellite imagery based on association of identified spatial patterns and features common to both known mine sites and new areas of interest. We plan to tie the re-picked and re-located seismicity to these mine locations. Future work where we will use our assembled GT information includes mining explosion discrimination studies, traveltime correction surface refinement, and azimuth correction surface estimation.

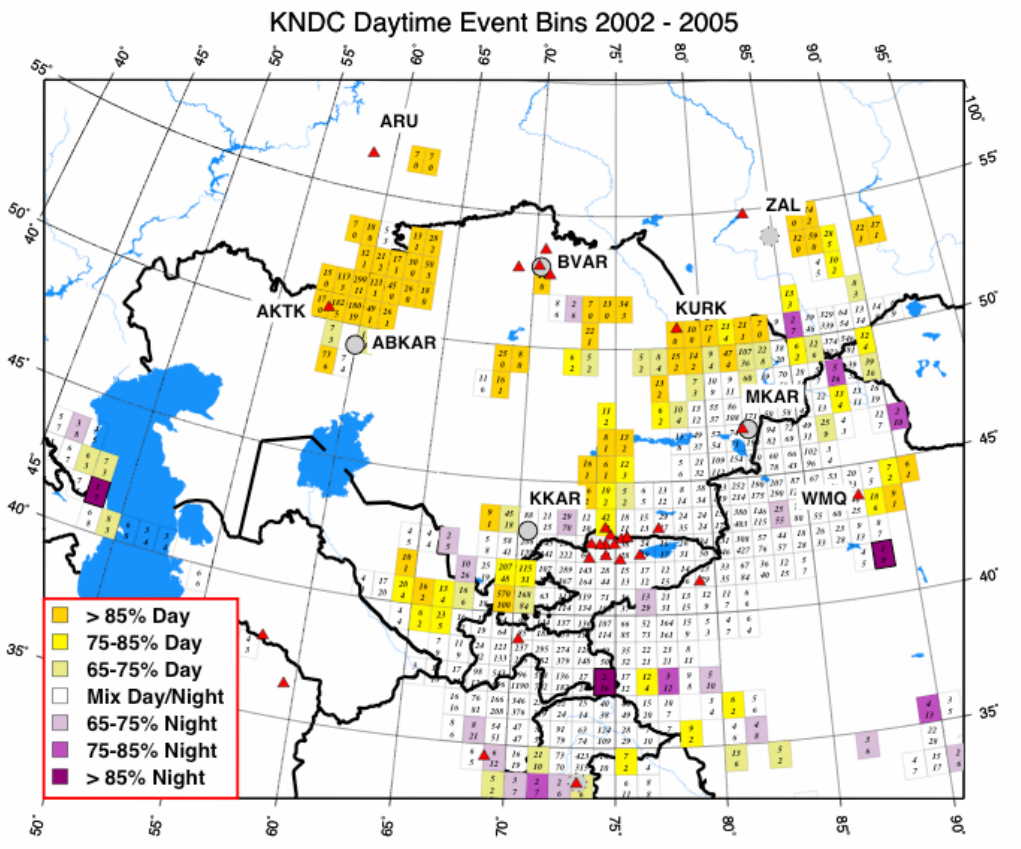

Figure 8. Time-of-day bins for KNDC seismicity.

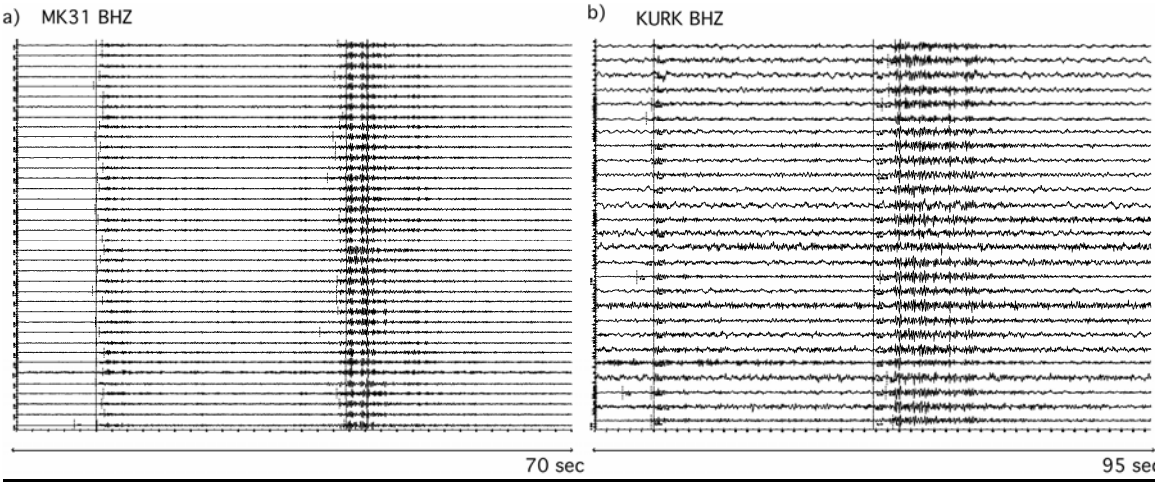

Figure 9. Correlated seismic events in Central Asia, presumed to originate at a mine. Aligned waveforms from stations MK31 (a) and KURK (b) are shown.

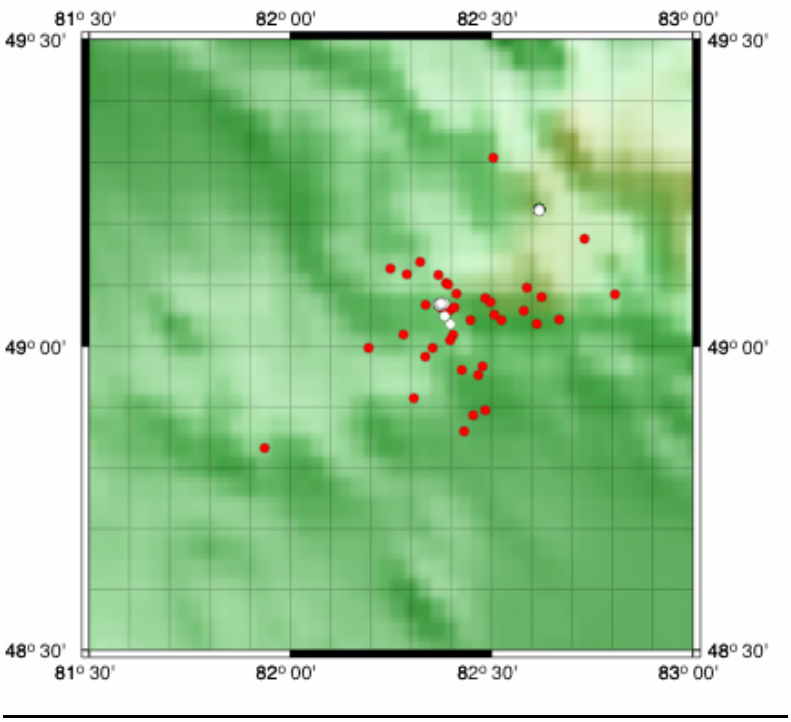

Figure 10. Catalog locations (red circles) and our relocations using correlation picks (white circles).

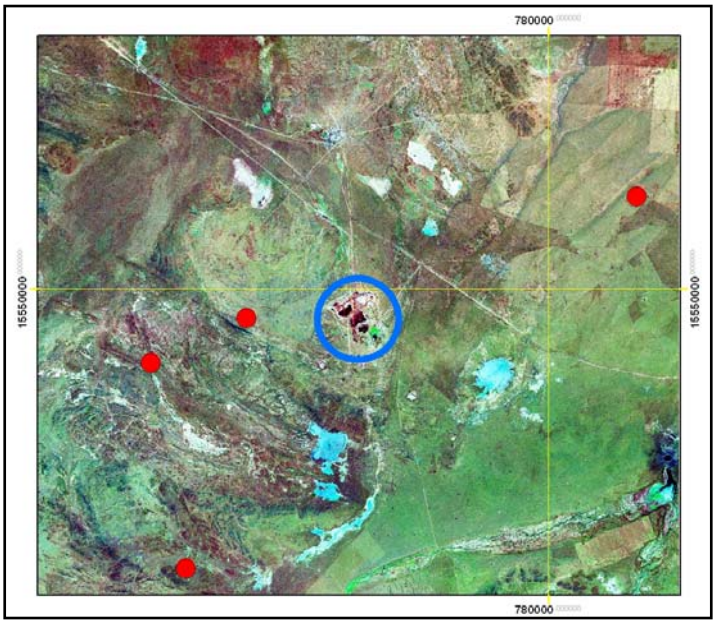

Figure 11. Satellite image showing a mine location in Central Asia. Red circles are catalog seismic locations.

CONCLUSIONS AND RECOMMENDATIONS

We continue to expand our research efforts to improve discrimination and location in Asia. We present new methods of model development that improve location ability in Asia. In addition, synergistic efforts combining seismics, satellite imagery and pattern recognition software show great promise. We recommend these efforts be continued and expanded.

ACKNOWLEDGEMENTS

We gratefully acknowledge valuable discussions with Howard H. Patton.

REFERENCES

Birch, F. (1961). The velocity of compressional waves in rocks to 10 kilobars, Part 2, *J. Geophys. Res.* 66: 2199–2224.

Christensen, N. I. and W. D. Mooney (1995). Seismic velocity structure and composition of the continental crust: A global view, *J. Geophys. Res.* 100: 9761–9788.

Julià J., C. J. Ammon, R. B. Herrmann, and A. M. Correig (2000). Joint inversion of receiver function and surface wave dispersion observations, *Geophys. J. Int.* 143: 99–112.

Liang, C., X. Song, and J. Huang (2004). Tomographic inversion of Pn travel times in China, *J. Geophys. Res*. 109: B11304, doi:10.1029/2003JB002789.

Maceira, M., S. R. Taylor, C. J. Ammon, X. Yang, and A. A. Velasco (2005). High-resolution Rayleigh wave slowness tomography of central Asia, *J. Geophys. Res.* 110: B06304, doi:10.1029/2004JB003429.

Nafe, J. E., and C. L. Drake (1963). Physical properties of marine sediments, in *The Sea*, Vol. 3, edited by M. N. Hill, pp. 794–815: Interscience, New York.

Onizawa, S., H. Mikada, H. Watanabe, and S. Sakashita (2002). A method for simultaneous velocity and density inversion and its application to exploration of subsurface structure beneath Izu-Oshima volcano, Japan, *Earth Planets Space*, 54: 803–817.

Phillips, W. S., C. A. Rowe, and L. K. Steck (2005), The use of interstation P wave arrival time differences to account for regional path variability, *Geophys. Res. Lett.* 32: L11301, doi:10.1029/2005GL022558.

Rowe, C.A., R. C. Aster, B. Borchers, and C. J. Young (2002), An automatic, adaptive algorithm for refining phase picks in large seismic data sets, *Bull. Seismol. Soc. Amer.* 92: 1660–1674.

Rowe C., H. Thurber, and R. A. White (2004). Dome growth behavior at Soufriere Hills Volcano, Montserrat, revealed by relocation of volcanic event swarms, 1995-1996, *Jour. Volc. Geotherm. Res.* 134: 199–221.

Rowe, C., L. Steck, W. Phillips, M. Begnaud, R. Stead, H. Hartse, K. Mackey, and K. Fujita (2006). Pn tomography and location in Eurasia, Proceedings, 24th General Assembly of the International Association of Seismology and Physics of the Earth's Interior, October, 2005, Santiago, Chile.

Steck, L.K., Rowe, C.A., W.S. Phillips, H. Hartse, K. Mackey, and K. Fujita (2005). Differential travel-time Pn tomography in northeast Asia, *EOS*, Transactions, AGU. 86: (52), Fall. Meet. Suppl., Abstract T54A-02.

Sun, Y. and M. N. Toksöz (2006). Crustal structure of China and surrounding regions from P wave traveltime tomography, *J. Geophys. Res*. 111: doi:10.1029/2005JB003962.

Tapley, B., J. Ries, S. Bettadpur, D. Chambers, M. Cheng, F. Condi, B. Gunter, Z. Kang, P. Nagel, R. Pastor, T. Pekker, S. Poole, and F. Wang (2005). GGM02 - An improved Earth gravity field model from GRACE, *J. Geodesy*, DOI 10.1007/s00190-005-0480-z.